Characterization of Asphaltene Using Potential Energy and Nanocalculation

Sabbaghi, Samad; Jahanmiri, Abdolhossein*+; Ayatollahi, Shahaboddin
Department of Chemical Engineering, Shiraz University, Shiraz, I.R. IRAN

Shariaty Niassar, Mojtaba
School of Chemical Engineering, University College of Engineering, University of Tehran, Tehran, I.R. IRAN

Mansoori, Gholam Ali
Department of Chemical Engineering, University of Illinois, Chicago, USA

ABSTRACT: *The basics of quantum mechanics and statistical thermodynamics were used to predict the potential energy and intermolecular forces of asphaltene molecules. The parameters associated with the chemical structure were also estimated for a specific asphaltene molecule to predict the Mie potential function. Based on the structural results, a new form of the Virial EOS with Peneloux correction was developed to estimate the density, solubility parameter and a correction factor that accounts for the structural effect of asphaltene. In this way, asphaltenes were considered as polymer-like compounds consisting of aggregates of a monodisperse. Finally, three new correlations were developed to predict the key parameters of asphaltenes, namely structural coefficient, density and solubility as functions of temperature and molecular weight. The correlations facilitate the calculation of the numerical methods of these parameters. These parameters were also compared successfully with the results found by the Soave Redlich Kwong equation of state. Meanwhile, at first the stage asphaltene was extracted and the roughness of the asphaltene coating in different rpm was studied by using of image analysis confocal microscopy.*

KEY WORDS: *Modeling, Asphaltene, Nanotechnology, Intermolecular forces, Potential energy.*

INTRODUCTION

Heavy oils and bitumen contain a mixture of hydrocarbons with complex structures of polyaromatic rings and short side chains known as asphaltene. In general, the high molecular weight asphaltene is the most aromatic fraction with the highest number of side chains and the low molecular weight asphaltene contains the lowest number of side chain, while the number of side chain of the whole asphaltene fraction lies in between. Remediation of the heavy organic deposits in the course of petroleum production has been a costly process and it

* To whom correspondence should be addressed.
+ E-mail: jahanmir@shirazu.ac.ir
1021-9986/08/2/47 12/$/3.20

has hampered the production activities in many parts of the world. Precipitation of asphaltene in wells and reservoirs has detrimental effects on the economics of oil production as it reduces well production. On the other hand, using the knowledge of exact intermolecular interactions between molecules and development of accurate nanoscale phase separations/transition models, it will become possible to increase our fundamental understanding of organic nanostructures.

ASPHALTENE STRUCTURE

The investigation of the chemical constitution of petroleum heavy fractions such as asphaltene is hindered by their complex nature. The need for understanding the nature of heavy organics in crude oil and their role in production and processing of petroleum is well recognized around the world as manifested by the extensive related researchers, while the experimental activities are still underway at various research centers [1-4]. Since 1980's many models of asphaltene precipitation have been developed to predict the onset and the amount of asphaltene precipitation. These predicting models can be divided into five groups (Solubility, solidarity, equation of state, colloidal and micellization model) [5-11].

The models will be improved very well if the structure of asphaltene is known. However the asphaltenes structures are hardly known. There have been considerable efforts by analytical chemists to characterize asphltene in terms of chemical structure, elemental analysis as well as their carbonaceous sources. A number of investigators have attempted to postulate model structures for asphaltenes based on physical and chemical methods that are for local oils. Fig. 1 shows the molecular structure of asphaltene proposed for 510 °C residue of Venezuelan crude [12].

The nano scale is increasingly becoming very important in today's advancing technology. It is strongly focused towards new nanoscale devices, which will benefit in all sorts of applications in the near future. The promise and the essence of nanoscale science and technology is based on a fact that materials at the nanoscale have properties (i.e., chemical, electrical, magnetic, mechanical, and optical) quite different from those of the macroscale. Some of these properties are, somehow, intermediate between the smallest elements

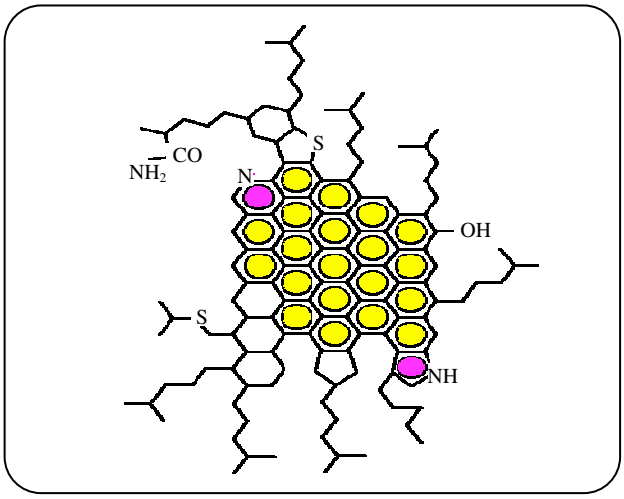

Fig. 1: Molecular structure of asphaltene [12].

(atoms and molecules) and those of the macroscopic materials. Compared to bulk materials, it is demonstrated that nanoparticles possess enhanced performance properties when they are used in similar applications. There are many present and expected applications of nanotechnologies including bottom-up technology (such as self-assembly) in biology, medicine, pharmaceuticals, electronics, energy, and environmental industries, which are rapidly increasing [13, 14]. Aggregation and growth of asphaltenes in crude oils of different stability were studied using confocal microscopy [15-17].

CONSTRUCTION OF MODEL FOR ASPHALTENE

Asphaltene particles are believed to exist in petroleum partly dissolved and partly in steric-colloidal and / or micellar forms depending on the polarity of their oil medium and presence of other oil compounds. In the last few years, the precipitation, flocculation and deposition of these molecules have been characterized and analyzed [18,19]. Small-size asphaltene particles may be dissolved in a petroleum fluid, whereas relatively large asphaltene particles may flocculate out of the solution, due to high paraffin content of the oil, forming random flocs as shown in Fig. 2. Due to their large size and their adsorption affinity to solid surfaces, asphaltine flocs (random aggregates) can cause quite stable deposits which may not wash away by current remediation techniques. Asphaltene flocs can form steric-colloids in the presence of excess amounts of resins and paraffin hydrocarbons as shown in Fig. 3 [19, 20].

Most of these investigations are indicative of the fact that asphaltene particles may self-associate, but not flocculate, and form micelles in the presence of aromatic hydro-carbons (or other polar solvents) as shown in Fig. 4.

PREPARATION OF ASPHALTENE AND COATED SILICON WAFERS

Experiments were performed to determine the amounts of asphaltenes precipitated with n-heptan. The titration experiments consisted of adding a volume of *n*-heptan, corresponding to a specific titrant-oil ratio, to the amount of sample in an appropriate flask. After 10 min of ultrasonic shaking, the mixture was left overnight. The solution of *n*-heptan and deasphalted oil was filtered using a vacuum system with a 0.45 μm filtration teflon membrane (previously weighed). The flask and the filtration membrane were rinsed with small volumes of the corresponding *n*-heptan to eliminate the residual oil. The membrane with the precipitated material was dried in a vacuum oven at 0.1 bar (gauge pressure) and 333 K over 6 hours and finally weighed to determine the asphaltene mass precipitated. Silicon wafers were cut into 1.5×1.5 cm square pieces and used as the substrates for the preparation of asphaltene-coated surfaces. In each test, the cut wafers were first cleaned with chloroform in an ultrasonic bath for 10 min in an attempt to remove all organic surface contaminants. An asphaltene-in-toluene stock solution of 1.0 mg/ml concentration was prepared. This solution was centrifuged at 2×10^4 rpm for 20 min to remove any inherent fine solids. In this experiment, samples from the top of the centrifuge tube were used in the spin coating of asphaltenes on the silicon wafers. The spin coating was performed at 10^3 and 3×10^3 rpm. The properties of oil used in this study are listed in table 1.

The silicon wafer coated with asphaltene, are shown in Figs. 5 and 7, respectively [17]. The following images were the first obtained using the Explorer scanning probe microscope operating on contact mode. The projection of lines (1-3) is displayed in Figs. 6 and 8 and the results are tabulated in table 2. Comparing the obtained result, one can conclude that the thickness and abrasion of the coated layer are inversely proportional to the spin velocity. The result is obtained for mean height parameters. Regarding this observation, high velocity spinning is employed to get a smooth sample. Since for the measurement of Van Der Waals (VDW) forced coating is required, it is

Table 1: Crude oil properties.

Sample of oil			
Mineral material percent	9.5 %	Organic material percent	90.5 %
Na	0.23 %		
K	0.04 %		
Fe	6.18 %	Asphaltene &	
Ca	0.36 %	Resins	54.4 %
Mg	0.16 %		
Si	0.38 %		
So_4^{-2}	2.15 %	Wax	36.1 %

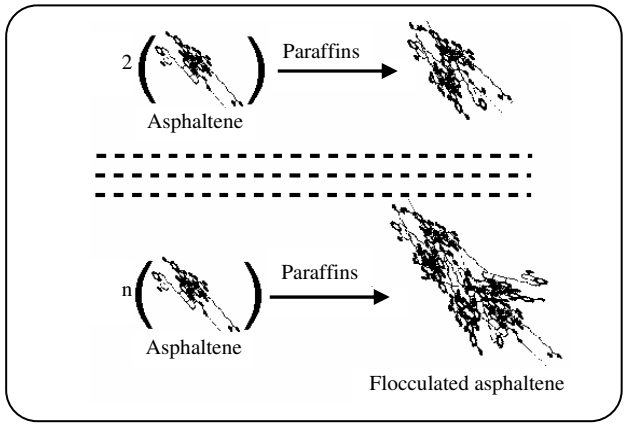

Fig. 2: Asphaltene flocculation.

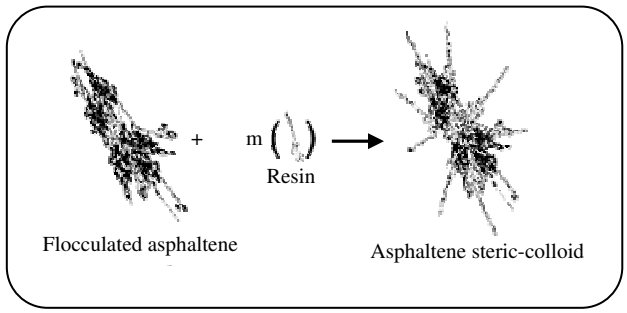

Fig. 3: Asphaltene steric-colloid formation from flocculated asphaltene.

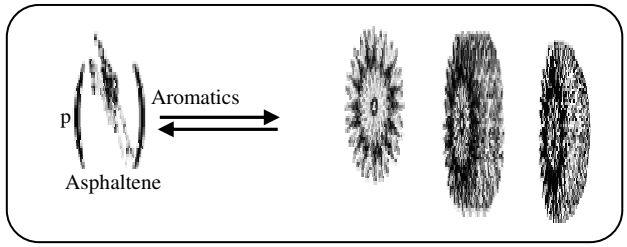

Fig. 4: Micelle formation in the presence of aromatics.

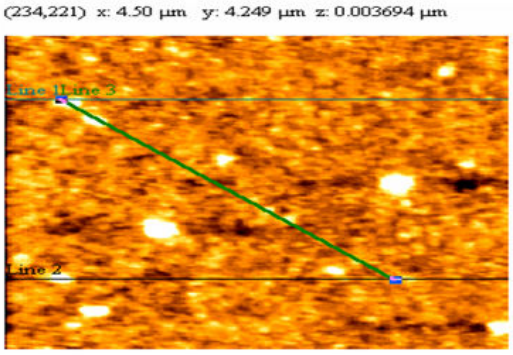

Fig. 5: Line profile plot on AFM asphaltene image.

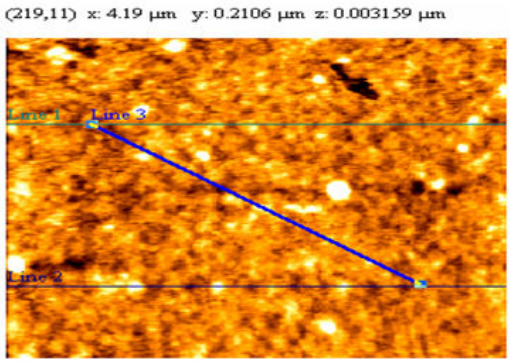

Fig. 7: Lines profile plot on asphaltene coated silicon wafer.

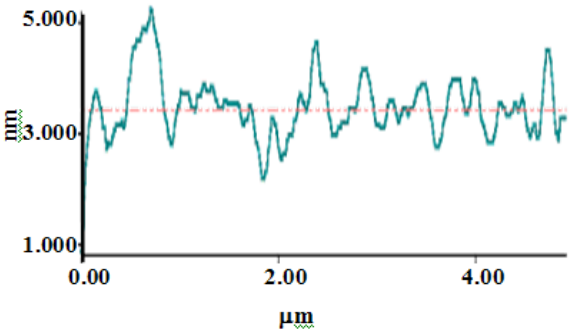

Fig. 6a: Confocal image of line 1 for crude oil.

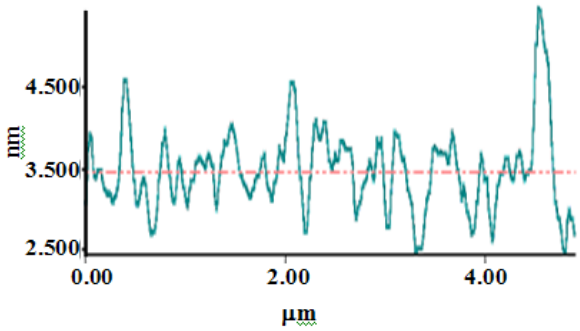

Fig. 8a: Confocal image of line 1 for crude oil.

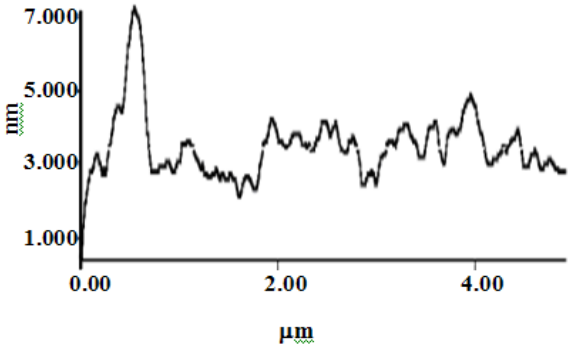

Fig. 6b: Confocal image of line 2 for crude oil.

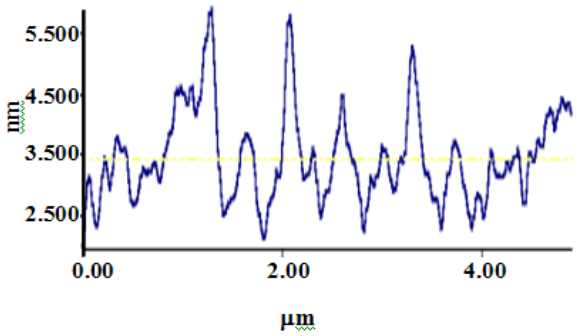

Fig. 8b: Confocal image of line 2 for crude oil.

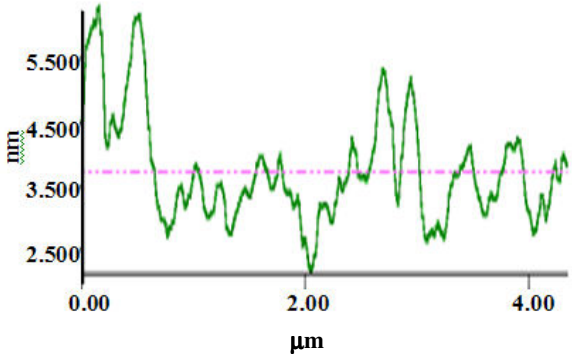

Fig. 6c: Confocal image of line 3 for crude oil.

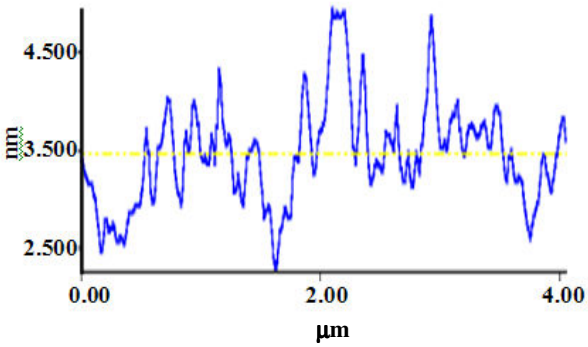

Fig. 8c: Confocal image of line 3 for crude oil.

Table 2: AFM results for the roughness average of asphaltene coating at different rpm.

	1000 rpm	3000 rpm
Line 1	0.4034 nm	0.3608 nm
Line 2	0.6105 nm	0.5750 nm
Line 3	0.6528 nm	0.3943 nm

necessary that the layer be thin enough, so that the interaction forces can be easily detected.

COMPUTATIONAL DETAILS OF THE PROPOSED MODEL

The interaction of forces between molecules in macromolecules is very critical and can not be ignored. These systems are dense and molecules are very near to each other such that most of their properties are governed by these interaction forces.

It has been shown that measurable macroscopic quantities are related to microscopic interactions between molecules. For the calculation of chemical potential, complicated numerical calculations are needed that can be evaluated by quantum mechanics. A rather general function used in interaction potential energy is the Mie potential function [21, 22].

$$U(r)=\frac{n\varepsilon}{n-m}\left(\frac{n}{m}\right)^{\frac{m}{n-m}}\left[\left(\frac{\sigma}{r}\right)^{n}-\left(\frac{\sigma}{r}\right)^{m}\right] \qquad (1)$$

The constants ε and σ are obtained from potential energy data. To find the best function for potential energy, a structure for the asphaltene was first proposed and the molecular dynamic method was used to calculate the chemical potential as a function of distance between the atoms. The method of semi-empirical equations and PM3 are used to calculate the parameters associated with the chemical structure. This solves an approximate form of the Schrodinger equation that depends on having appropriate parameters available for the type of chemical system in the question [21-25]. Our previous work showed that, a proposed model for the potential energy of asphaltene resulted in good agreement with the calculated parameters from EOS [3].

The validity of the result has been checked by comparing the results predicted by the model with the calculated data. The results are then used to investigate the behavior of asphaltene. In order to determine the constants of the potential function, the calculated data have been fitted. The results are shown in table 3.

Table 3: Parameters for Eq. (1).

Constant	Value
n	18
m	9
σ	16.0399
ε	23.057

The curve of potential energy (U) versus distance (r) is drawn in Fig. 9 by using the proposed function of potential energy.

SECOND-VIRIAL COEFFICIENT

Eq. (2) shows a general form of Virial equation:

$$\frac{PV}{RT}=1+\frac{B_2(T)}{V} \qquad (2)$$

Here the second-Virial coefficient $B_2(T)$ is a function of temperature which can be obtained by the interaction between pairs of molecules. Previous works using the statistical mechanics showed that the second-Virial coefficient for potential energy can be calculated by [21]:

$$B_2(T)=-2\pi\int_0^{\infty}\left(e^{-\beta U}-1\right)r^2dr \qquad (3)$$

Where;

$$\beta=\frac{1}{KT} \qquad (4)$$

Fig. 10 shows the second-Virial coefficient as a function of temperature based on Eq. (3). These results were fitted using an exponential model with Eq. (5) and constant values shown in table 4.

$$B_2(T)=xe^{yT} \qquad (5)$$

A MODIFIED FORM OF THE VEOS FOR ASPHALTENE

It is proved that the VEOS, with a Peneloux correction gives the best estimates of the liquid molar volume obtained as follows [26]:

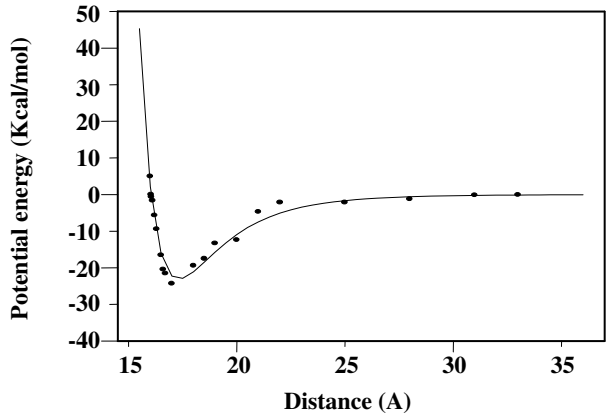

Fig.9: Potential energy of asphaltene vs. distance using Eq. (1) (Line Eq. (1), (●) quantum mechanic [3]).

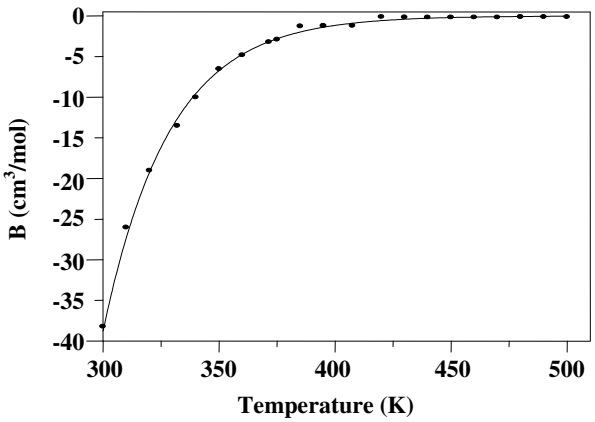

Fig. 10: Second-Virial coefficient vs. temperature for asphaltene using Eq. (5) (Line the Eq. (5); (●) Eq. (3)).

$$V^{L} = V^{Virrial} - C \tag{6}$$

Where C is the Peneloux correction term which can be estimated by:

$$C = 1.374(MW)^{1.27}(.29 - Z_{RA}) \tag{7}$$

Where Z_{Ra} is the Racket compressibility factor proposed by Spencer and Danner for saturated liquid molar volume [27]. This can be calculated using the following correlations, presented by *Reid et al.* [28].

$$Z_{RA} = 0.29 - 0.088\omega \tag{8}$$

$$W = C_f\left[0.584\ \ Ln(MW) - 2.54\right] \tag{9}$$

Replacing V in Eq. (2) by $V^{Virrial}$ of Eq. (6) will result in the following form of the EOS:

$$P = \frac{RT}{\left(V^{L} + C\right)}\left(1 + \frac{B_2(T)}{\left(V^{L} + C\right)}\right) \tag{10}$$

If $\bar{r}$ is defined as the average number of monomers in a given aggregate, then the parameters of Eq. (10) for the aggregates related to the monomer parameter will be [29]:

$$\bar{r} = \frac{\overline{MW}^{agg}}{MW^{mon}} \tag{11}$$

$\overline{MW}^{agg}$ and MW^{mon} are the average molar mass of the asphaltene aggregate and the monomer molar mass, respectively.

$$C = \bar{r}\, C_m \tag{12}$$

$$B = \bar{r}\, B_m \tag{13}$$

$$V^{L} = \bar{r}\ v^{L} \tag{14}$$

Where C_m and B_m are the monomer parameters. This idea was first suggested by *Sy-Siong-Kiao et al.* [30] and later applied by *Akbarzadeh et al.* [9-11, 29, 31]. The modified VEOS is obtained by replacing C in Eq. (10):

$$P = \frac{RT}{\bar{r}\left(v^{L} + C_m\right)}\left(1 + \frac{B_m}{\left(v^{L} + C_m\right)}\right) \tag{15}$$

First the density of asphaltene was calculated using modified VEOS (Eq. 15) [32]. The temperature effects on the predicted density of asphaltene by modified VEOS for different molecular weights are shown in Fig. 11. It is shown that as the temperature increases, the density of asphaltene decreases. The results shown in Fig. 11 include the effects of the molecular weight on the density of asphaltene, which shows the trend of density changes as the molecular weight increases. The calculated density of asphaltene using SRK EOS [29] is also added to Fig. 11 for the sake of comparison. This indicates the ability of the VEOS for the prediction of asphaltene density.

EOS CALCULATION OF SOLUBILITY PARAMETER

The solubility parameter, one of the key parameters in modeling asphaltene behavior, could be estimated either by a correlation or an EOS. Here, we have used the modified form of the VEOS to derive a relation for estimating the solubility parameter of asphaltene. *Hildebrand, et al.* correlated the liquid solubility parameter of non-polar solvents (δ^{L}) to the internal energy of

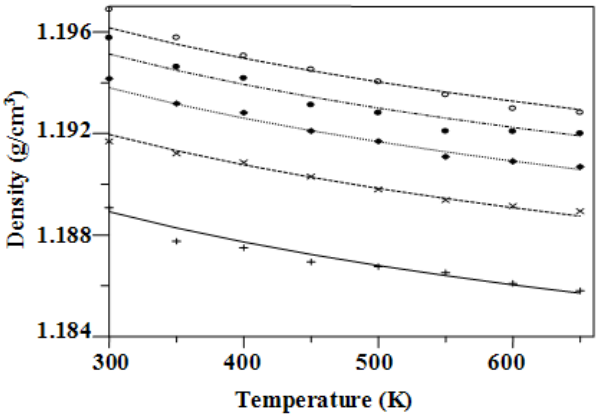

Fig. 11: Density vs. temperature for asphaltene using Eq. (15) compared to SRK EOS [29]; (○) MW = 9200; (●) MW = 7400; (♦) MW = 5600; (×) MW = 3800; (+) MW = 2000; (Lines Eq. (2), symbols SRK EOS).

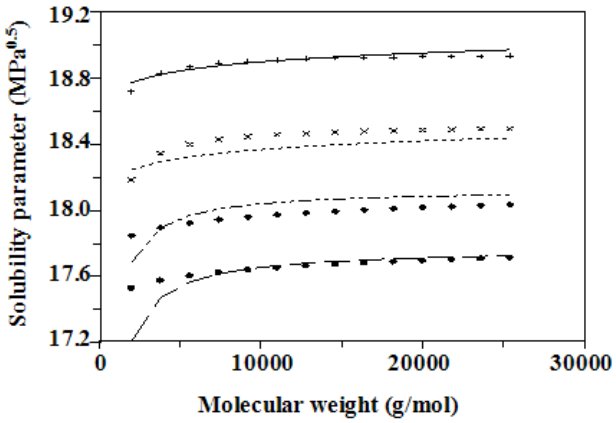

Fig. 12: Solubility parameter vs. temperature for asphaltene using Eq. (18) compared to SRK EOS [29]; (+) 300 K; (×) 400 K; (♦) 500 K; (●) 600 K; (Lines Eq. (18), symbols SRK EOS).

vaporization (ΔU^{LV}) and the molar volume of the liquid phase (v^L) to obtain [33]:

$$\delta^L = \left(\frac{\Delta U^{LV}}{v^L} \right)^{\frac{1}{2}} \tag{16}$$

The internal energy of vaporization was calculated using the following equation [28]:

$$\Delta U^{LV} = \int_{v^l}^{v^v} \left[\left(T \frac{\partial P}{\partial T} \right)_v - P \right] \cdot dv \tag{17}$$

Therefore, the solubility parameter can be obtained by Eqs. (16) and (17), that is:

$$\delta^L = \frac{T}{v^l} \left[R \frac{dB}{dT} \right]^{1/2} \tag{18}$$

Note that the number of monomers ($\bar{r}$) indirectly affects the solubility parameter (Eq. (18)) as the monomer molar volume, (v^L) determined from Eq. (15), is a function of ($\bar{r}$). The calculated solubility parameters by VEOS using Eq. (18) are plotted in Fig. 12, where the predicted solubility parameter of asphaltene is plotted versus the molar mass for different temperature.

As is shown here, the molar mass has little effect on the solubility parameter of asphaltene. For liquids, temperature affects both the internal energy of vaporization and density. The changes in these properties result in a decrease in the solubility parameter of asphaltene. Fig. 12 also compares the calculated solubility of asphaltene from the proposed model with the results of SRK EOS [29].

To clearly show the compatibility between these two EOS in predicting solubility parameters, Fig. 13 compares the solubility parameter calculated from the model (VEOS) with SRK EOS [29]. According to Fig. 13, all the points scatter around the 45-degree line, which means good agreement has been achieved here. To check the accuracy of the proposed model, the density measurements at different temperatures are also calculated.

INTERMOLECULAR FORCES

It should clearly be understood that all the forces between atoms and molecules are electrostatic in origin. They are ultimately based on Coulomb's law of attraction between unlike, and repulsion between like charges. The interparticle interaction potential energy between molecules is generally denoted by [21, 22]:

$$U(r) = U_{rep.} + U_{att.} \tag{19}$$

Interparticle energies are known to be orientation dependent and are the sum of repulsive, London dispersion, hydrogen bonding as well as electrostatic energies. For natural and spherically symmetric molecules when the separation distance (r) is large, the London dispersion forces dominate. Then all these forces may be represented as gradients of potential energies [21].

$$F = -\partial U / \partial r = F_{rep.} + F_{att.} \tag{20}$$

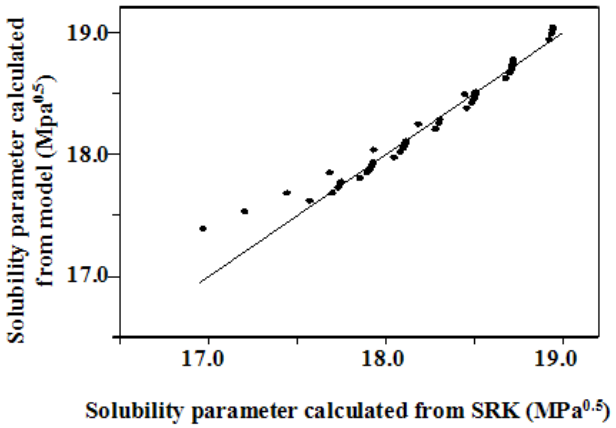

Fig. 13: Solubility parameter comparison with SRK EOS results [29].

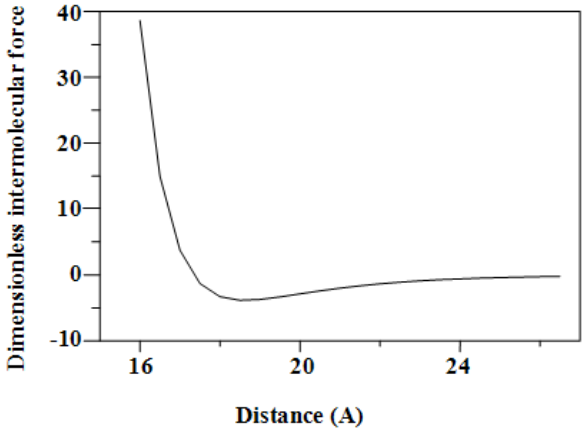

Fig. 14: Dimensionless force vs. distance.

Total force is calculated by Eq. (20) and then a plot of dimensionless force $\xi = F\sigma/\varepsilon$ versus distance is shown in Fig. 14.

SHIFTED-FORCE POTENTIAL

For testing purposes, the step change in U(r) and F(r) can be removed by shifting F(r) vertically. So, the force goes smoothly to zero at r_c. Hence, define a shifted force $F_S(r)$ by [34]:

$$F_s(r) = \begin{cases} -\dfrac{dU}{dr} + \Delta F & r \subseteq r_c \\ 0 & r \supset r_c \end{cases} \qquad (21)$$

Where ΔF is the magnitude of the shift.

$$\Delta F = -F(r_c) = \left(\frac{dU}{dr}\right)_{r_c} \qquad (22)$$

The shifted- force potential ($u_s(r)$) corresponding to $F_S(r)$ can be derived from:

$$F_S(r) = -\frac{dU_S(r)}{dr} \qquad (23)$$

$$\int_o^{u_S} dU_S = -\int_\infty^r F_S(r).dr \qquad (24)$$

Substituting Eq. (21) into Eq. (24) and integrating gives:

$$U_s(r) = \begin{cases} U(r) - U(r_c)(r - r_c)\left.\dfrac{du}{dr}\right|_{r=r_c} & r \subseteq r_c \\ 0 & r \supset r_c \end{cases} \qquad (25)$$

Eq. (26) and Fig. 15 compares this shift force potential with proposed model.

$$U_S(r) = U(r) + 0.0125 \times r - 0.45 \qquad (26)$$

RESULTS AND DISCUSSION

The validity of the results has been checked by comparing the results predicted by the model with the calculated data. It showed a good agreement which was promising. Then, the results were used to investigate the behavior of asphaltene. The numerical results are shown in table 5.

A dimensionless potential function was proposed for the sake of generality of the results. The comparison between intermolecular forces and the potential function is shown in Fig. 16. So, dimensionless shifted-potential energy (U^*) and dimensionless distance (r^*) was expressed to facilitate working a comparison between the results shown in this paper. Therefore, dimensionless potential and distance are defined by Eqs. (27),(28) and the result is graphically shown in Fig. 17.

$$U^* = \frac{U_s}{\varepsilon} \qquad (27)$$

$$r^* = \frac{r}{\sigma} \qquad (28)$$

The calculated key parameters of asphaltene presented in Figs. 11 and 12 clearly indicate the effects of molar mass and temperature on density and solubility. We then developed three correlations for prediction of density, the solubility parameter and the structure coefficient,

Table 4: Parameters for Eq. (5).

Constant	Value	Unit
X	-1407780.7	$cm^3.mol^{-1}$
Y	-.035	K^{-1}

Table 5: Potential energy of asphaltene for the proposed the model.

r(A)	U(r) Calculated	U(r) Model
16	3	2.138129
16.04	-.006	-.00532834
16.05	-.637	-.5182515
16.1	-1.644	-2.951863
16.2	-5.680	-7.212301
16.3	-9.425	-10.75559
16.5	-16.55	-16.06854
16.6	-20.455	-17.99689
16.7	-21.532	-19.52859
17	-24.323	-22.26625
18	-19.4	-21.09931
18.5	-17.5	-18.46506
19	-13.315	-15.71186
20	-12.395	-10.92182
21	-4.699	-7.438375
22	-2.133	-5.056317
25	-2.115	-1.667821
28	-1.221	-.6086506
31	-.165	-.2444973
33	-.0695	-.1394446

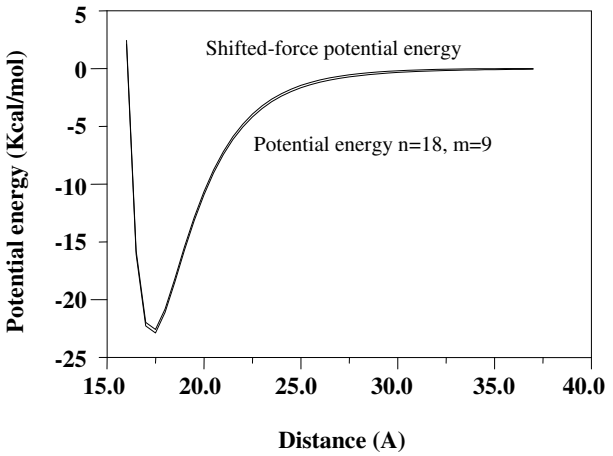

Fig. 15: Comparison of the model with shifted-force potential.

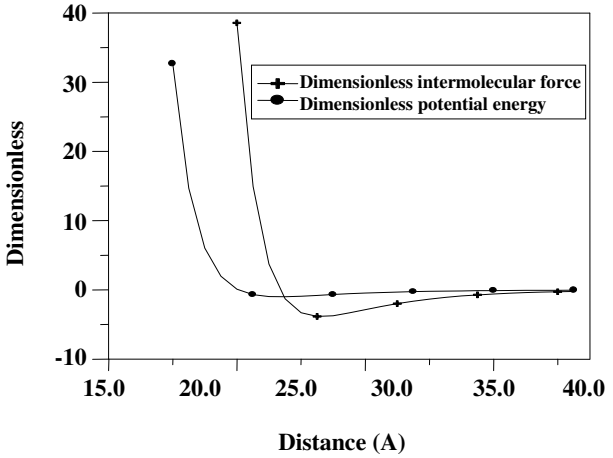

Fig. 16: Dimensionless intermolecular force and potential energy vs. distance.

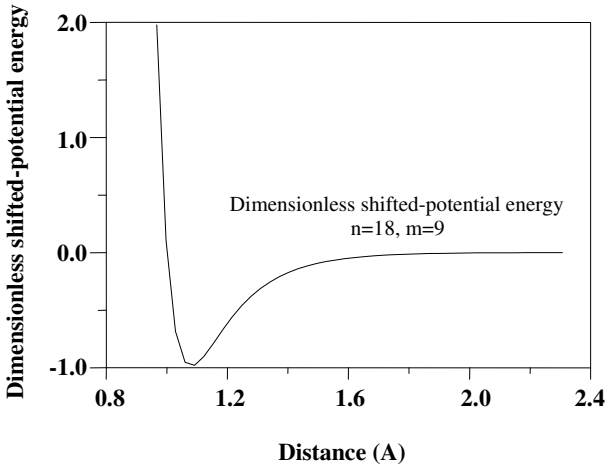

Fig. 17: Dimensionless potential energy vs. distance.

respectively. The structure coefficient, as a key parameter in the VEOS, was predicted through the back calculation of the densities from SRK EOS. This scenario proceeds from Eqs. (6)-(9) towards Eq. (15), resulting in the C_f calculation at different temperatures, as well as asphaltene molecular weight.

To summarize, three new correlations are presented here to estimate the structure coefficient, density and solubility parameter of asphaltene. The developed correlations are presented in Eqs. (29)-(31) as functions of temperature and molecular weight. Besides the structure of the asphaltene, the theory of quantum mechanics was used to predict these correlations, enabling us to use them in the simulator exclusively without trial and error.

$$\rho = 1.1767(MW)^{0.00398}(T)^{-0.0035} \quad (29)$$

$$\delta = 32.02(MW)^{0.0041}(T)^{-0.0991} \quad (30)$$

$$C_f = 182.74(MW)^{-1.1677}(T)^{1.13}\left(\frac{\overline{H}}{rpm}\right)^{0.125} \quad (31)$$

$$\overline{H} = \frac{\sum_{i=1}^{N} H_i}{N} \quad (32)$$

Figs. 18 and 19 show the density, solubility parameters and structure coefficient as functions of molecular weight and temperature calculated from Eqs. (29)-(31) respectively. According to these results, density increases sharply with the increase in molecular weight, before approaching a constant value at very high molecular weight. The solubility parameter of asphaltene is not sensitive to the molecular weight value, however its value decreases as the temperature increases as shown in Fig. 19. Fig. 20 shows structure coefficient versus molar weight of asphaltene using Eq. (31) at different temperatures.

CONCLUSIONS

A key theme of the paper is the application of nanotechnology in the analysis of asphaltene at the molecular structure. If intermolecular structure of a particle is known, then technically, one can predict its size by taking into account the bond lengths. It is understood that formidable challenges remain in the fundamental understanding of various phenomena in organic nanostructures before their impact on

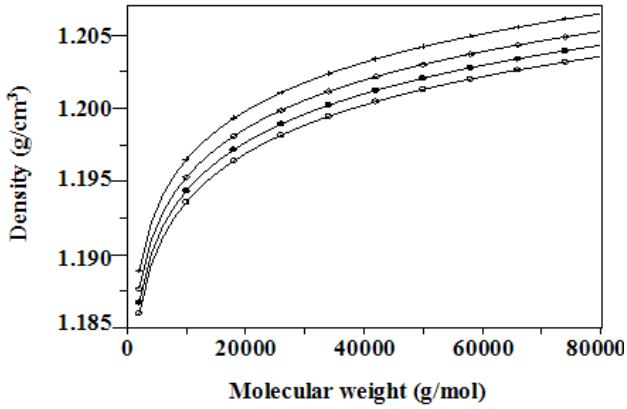

Fig. 18: Density vs. molar mass for asphaltene using Eq. (29) compared to model; (+) 300 K; (◊) 400 K; (●) 500 K; (○) 600 K; (Lines Eq. (29), symbols model (VEOS)).

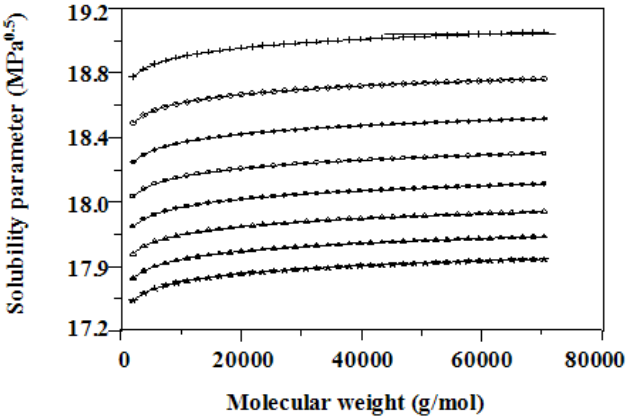

Fig. 19: Solubility parameter vs. molar mass for asphaltene using Eq. (30) compared to model; (+) 300 K; (◊) 350 K; (♦) 400 K; (○) 450 K; (●) 500 K; (△) 550 K; (▲) 600 K; (★) 650 K; (Lines Eq. (30), symbols model (VEOS)).

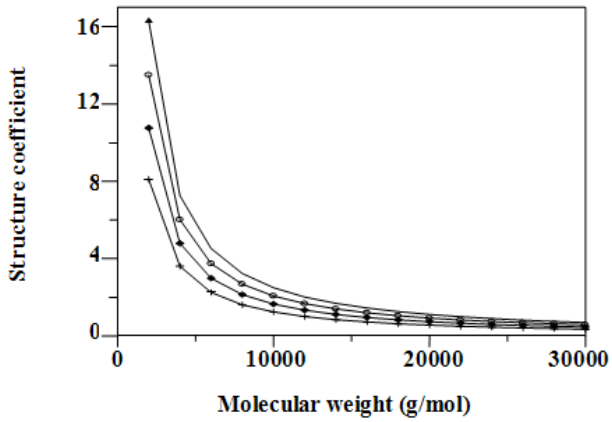

Fig. 20: Structure coefficient vs. molar mass of asphaltene using Eq. (31) at different temperatures; (+) 300 K; (♦) 400 K; (○) 500 K; (▲) 600 K.

nanotechnology becomes a reality. Using the knowledge of the exact intermolecular interactions between molecules and development of accurate nanoscale phase separations/transition models, it is possible to increase our fundamental understanding of organic nanostructures. Asphaltene at the molecular structure can have interesting and useful applications in nanotechnology. That is why in this research we tried to establish the details of the nanostructure of asphaltene for future nanotechnology application.

Our final goal was to observe and determine the surface structure of asphaltene micelles with the Explorer and Discoverer scanning probe microscopes. The unusual behavior of asphaltene molecules in petroleum fluids and in the model systems that use pure solvents and well-characterized asphaltene molecules were investigated. The focus of the work on such molecules are to characterize their structure, dynamics and thermo-dynamics, and to establish the relationship between these properties and petroleum fluid behavior. The focus of this work was to characterize the structure of heavy petroleum molecules, dynamics and thermodynamics to establish the relationship between these properties and petroleum fluid behavior.

Nomenclatures

List of symbols

$B_2(T)$	Second-Virial coefficient ($cm^3.mol^{-1}$)
B	Aggregate parameter
B_m	Monomer parameter
C	Peneloux correction
C_m	Monomer parameter
C_f	A correction factor that accounts for structural effect
$\overline{H}$	Mean *roughness*
K	Boltzmann constant ($Kcal.mol^{-1}.K^{-1}$)
$\overline{MW}^{agg}$	Average molar mass of the asphaltene aggregate ($g.mol^{-1}$)
MW^{mon}	Monomer molar mass ($g.mol^{-1}$)
MW	M olar mass of asphaltene ($g.mol^{-1}$)
m	Dimensionless constant of Eq. (1)
n	Dimensionless constant of Eq. (1)
p	Pressure (bar)
R	Universal gas constant ($bar.cm^3.mol^{-1}.K^{-1}$)
r	Distance ($\dot{A}$)
$\bar{r}$	Average number of monomer
T	Temperature (K)
U(r)	Potential energy ($Kcal.mol^{-1}$)
$U_{att.}$	The attractive energy ($Kcal.mol^{-1}$)
$U_{rep.}$	The repulsive energy ($Kcal.mol^{-1}$)
ΔU^{LV}	Energy of vaporization ($j.mol^{-1}$)
V	Volume (cm^3)
V^L	Molar volume of liquid ($cm^3.mol^{-1}$)
v^L	Monomer molar volume of liquid ($cm^3.mol^{-1}$)
V^{Virial}	Molar volume calculated by Virial Eq. ($cm^3.mol^{-1}$)
x	Parameter of Eq. (5) ($cm^3.mol^{-1}$)
y	Parameter of Eq. (5) (K^{-1})
Z_{RA}	Racket compressibility factor

Greek letters

β	Parameter of Eq. (3)
ε	Well depth ($Kcal.mol^{-1}$)
σ	Intermolecular distance at which the potential is zero ($\dot{A}$)
w	Acentric factor
δ	Solubility parameter(MPa^5)
Δ	Represents a change
ξ	Dimensionless force

Subscript

att.	Attractive
m	Monomer
rep.	Repulsive

Superscripts

L	Liquid
agg.	Aggregate
mon.	Monomer
Virial	Virial equation of state

Received : 11th February 2007 ; Accepted : 11th November 2007

REFERENCES

[1] David, A., *AIChE(Am. Inst. Chem. Eng.) Symp. Ser.*, **69** (127), 56 (1973).

[2] Lichaa, P.M., *Can. Pet. Tec. J.*, **Jun.**, 609 (1977).

[3] Sabbaghi, S., Jahanmiri, A., Shariaty Niassar, M., Ayatollahi, Sh. and Boushehri, A., *Int. J. Nanosci. & Nanotech.(IJNN)*, **1**, 31 (2005).

[4] Mansoori, G. A. and Jiang, T.S., Proc. 3rd Eur. Conf. on Enhanced Oil Recovery, Rome, (1985).

[5] Mansoori, G.A., *J. Pet. Sci. & Eng.*, **16**, 101, (1999).

[6] Andersen, S. and Speight, L., *J. Pet. Sci. & Eng.*, **22**, 53 (1999).

[7] Thomas, F.R., Bennion, D.W. and Hunter, RE., *Can. Pet. Tech.*, **31**, p.22 (1992).

[8] Alexander, G.L., Creagh, A. L. and Prausnitz, J. M., *Ind. Eng. Chem. Fund.*, **24**, 301 (1985).

[9] Akbarzadeh, K., Ayatollahi, Sh., Moshfeghian, M., Alboudwarej, H. and Yarranton, H.W., *J. Can. Pet. Tech.*, **43**, 9 (2004).

[10] Akbarzadeh, K., Ayatollahi, Sh., Nasrifar, Kh., Moshfeghian, M. and Yarranton, H.W., *Oil & Gas J.*, **44**, 28 (2002).

[11] Akbarzadeh, K., Ayatollahi, Sh., Moshfeghian, M., Alboudwarej, H., Svrcek, M. and Yarranton, H.W., 5th Int. Sym. on Thermodynamic of Heavy Oils and Asphaltenes, June 12-24, Calgary, Canada (2004).

[12] Carbognani, *INTEVEP S.A., Tech. Rept.*, (1992).

[13] Mansoori, G. A., World Scientific Pub., New York, (2005).

[14] Mansoori, G. A. and Fauzi Solaiman, T.A., *J. ASTM Int.*, **2**, 6, Paper ID JAL13110, (2005).

[15] Sabbaghi, S., Shariaty Niassar, M., Mansoori, G. A., Ayatollahi, Sh. and Jahanmiri, A., Energy Nano-technology Int. Conf., Jun 26-28, (MIT), Cambridge, MA (2006).

[16] Sabbaghi, S., Shariaty Niassar, M., Mansoori, G. A., Ayatollahi, Sh. and Jahanmiri, A., Nano Europe Fair & Conf., Sep. 12-14, Switzerland, Olma Messen St. Gallen, (2006).

[17] Sabbaghi, S., Ayatollahi, Sh., Shariaty Niassar, M., Jahanmiri, A., The MESM'2006 International Middle Eastern Multiconference on Simulation and Modeling, Alexandria 28-30, Alexandria, Egypt, (2006).

[18] Kawanaka, S., Leontaritis, K.J., Park, S.J. and Mansoori, G. A., ACS Symp. Ser. No. 396, Chapter 24, American Chemical Society, Washington, D.C., (1989).

[19] Mansoori, G.A., *J. Pet. Sci. & Eng.*, **17**, 101 (1997).

[20] Park, S. J. and Mansoori, G. A., *Energy Sources,* **10**, 109 (1988).

[21] Mc Quarrie, D.A., "Harper Collins Publishers", (1976).

[22] Hirschfelder, J. O., Curtiss, C. F. and Bird, R. B., "Molecular Theory of Gases and Liquids", 2nd Printing, Wiley, New York, (1964).

[23] Nyeland, C., *Che. Phy. Lett.*, **370**, 353 (2003).

[24] Akiyoshi, S., Satimi, K., Nobuaki, M. and Kenro, H., *Chem. Phys. Lett.*, **391**, 101 (2004).

[25] Yu Zhang, Shi. Hong-Yun, *J. Molecular Structure (Theochem)*, **589-590**, 89 (2002).

[26] Peneloux, A., Rauzy, E. and Freeze, R., *Fluid Phase Equilibria*, **8**, 7 (1982).

[27] Spencer, C.F. and Danner, R. P., *Chem. Eng. Data*, **17**, 236 (1972).

[28] Reid, R.C., Prausnitz, M. and Poling, B.E., "The Properties of Gases & Liquids", 4th Edition, Mc Graw-Hill, New York, (1989).

[29] Akbarzadeh, K., Ph.D. Dissertation, Dept. of Chem. Eng., Shiraz University, Iran, January, (2002).

[30] Sy Siong Kiao, R., Caruthers, L. M. and Chao, K. C., *Ind. Eng. Chem. Res.*, **35**, 1446 (1996).

[31] Akbarzadeh, K. and Moshfeghian, M., *Fluid Phase Equ*. **187-188**, 347 (2001).

[32] Sabbaghi, S., Shariaty Niassar, M., Ayatollahi, Sh. and Jahanmiri, A., *Fluid Dynamics & Materials Processing(FDMP)*, **105** (1), 1 (2008).

[33] Hildebrand, J., and Scott, R., "Solubility of Non-Electrolytes", 3rd Ed., Reinhold, New York, (2001).

[34] Nicolas, J., Gabbin, K. E. and Streett, W.B., *Mol. Phys.,* **37**,1429 (1979).